04. Brief Overview of Perovskite Oxide: Synthesis and Its Performance as Oxygen Separator from Air

by Silvana Dwi Nurherdiana

Submission date: 15-Mar-2022 08:56AM (UTC+0700)
Submission ID: 1784511067
File name: 04._Prosiding_Internasional-Brief_Overview.pdf (614.14K)
Word count: 5693
Character count: 29400

2nd International Conference Eco-Innovation in Science, Engineering, and Technology
Volume 2021
http://dx.doi.org/10.11594/nstp.2021.1412

NST PROCEEDINGS

OPEN ACCESS

Conference Paper

Brief Overview of Perovskite Oxide: Synthesis and Its Performance as Oxygen Separator from Air

Silvana Dwi Nurherdiana[1]*, Rachmad Ramadhan Yogaswara[1], Nove Kartika Erliyanti[1], Atika Nandini[1], Mutasim Billah[1], Sintha Soraya Santi[1], Hamzah Fansuri[2], Mohd Hafiz Dzarfan Othman[3,4], Yuly Kusumawati[2], Syafsir Akhlus[2]

[1]Department of Chemical Engineering, Engineering Faculty, Universitas Pembangunan Nasional "Veteran" Jawa Timur, Surabaya 60294, Indonesia
[2]Department of Chemistry, Faculty of Science and Data Analytics, Institut Teknologi Sepuluh Nopember, Kampus ITS Sukolilo, Surabaya 60111, East Java, Indonesia
[3]Advanced Membrane Technology Research Centre (AMTEC), Universiti Teknologi Malaysia, 81310 UTM Skudai, Johor Bahru, Johor, Malaysia
[4]Faculty of Petroleum and Renewable Energy Engineering, Universiti Teknologi Malaysia, 81310 UTM Skudai, Johor Bahru, Johor, Malaysia

*Corresponding author:
E-mail:
silvana.dwi.tk@upnjatim.ac.id

ABSTRACT

The aims of this brief overview are providing the knowledge about the physical and chemical properties of perovskite oxides in various synthesis method and the correlation of its performance for separating oxygen from air. Perovskite oxide showed excellent conductor of ion and electron, simultaneously through oxygen lattice in the crystal structure. In the present review, we have presented the detail on the crystal structure and the factor that affect the pseudo-crystal, various synthesis method i.e., solid-state, sol-gel, combustion, and co-precipitation. It has been completed with the discussion of the characteristic and the mechanism of the perovskite to separate oxygen from air

Keywords: Perovskite oxide, crystal structure, oxygen separator, catalyst

Introduction

Perovskite was firstly found in the Ural Mountain as a mineral in rocks with general structure such as calcium titanium oxide ($CaTiO_3$) which discovered by Gustav Rose in 1839 (Athayde et al.. 2015). Generally, the perovskite has a general structure of ABO_3. The A side may be filled by alkali and/or alkaline earth ions while the B side acts as an electron conductor and may be filled by transition metal ions or other metals which smaller than ions on A side (Teraoka et al, 1985 ; Zhou et al., 2009). The combination of metal ions and oxygen is generally shown in ideal symmetry of cubic crystal (P*m3m*) as shown in Figure 1. However, the the symmetry can also be distorted from cubic structure due to the effect of metal ion deposition in the perovskite structure.

The structure stability of a perovskite crystal greatly affects the performance especially at high temperature reaction such as POM reaction. While some crystal structure may can be distorted with the changes in temperature. A good structural stability is assessed from the unchanged structure during the reaction and the ion radius size of the A and B side remains at perovskite tolerance values between 0.8 and 1 which can be determined using Goldschmidt equation as shown in equation 1. Where R_A. R_B. R_O sequentially represents the radius of the ionic ions of A, B and O.

How to cite:
Nurherdiana, S. D., Yogaswara, R. R et al. (2021). Brief overview of perovskite oxide: synthesis and its performance as oxygen separator from air. *2nd International Conference Eco-Innovation in Science, Engineering, and Technology*. NST Proceedings. pages 68-79. doi: 10.11594/ nstp.2021.1412

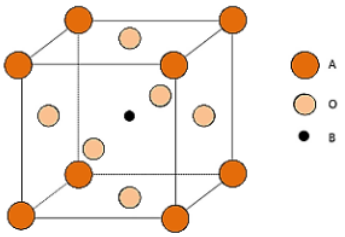

Figure 1. Cubic Structure (Pm3m) Perovskite Oxide.

On the other hand, the presence of oxygen vacancy in the perovskite structure and the stability of the structure, performance can be chemically affected by the oxygen ion diffusion. Hence, perovskite oxide has mixed ionic and electronic conductivity (MIEC) properties, where ion oxygen (O^{2-}) and electron diffused simultaneously to balance the charge. The presence of cations with large ionic radius causes a change of MIEC properties which can increase the mobility of oxygen ions (Möbius et al., 2009).

$$t = \frac{R_A + R_O}{\sqrt{2}(R_B + R_O)} \quad (1)$$

The oxygen ions pass through the ceramic membrane from high pressure to the other side of the membrane with low pressure. Oxygen on the high pressure will be adsorbed on the membrane surface to obtain two electrons and dissociates into oxygen ions which fill the oxygen vacancy side in the structure. The oxygen ion then migrates to the other side and at the same time, metal ions of the B side are oxidized to a higher valence state to balance the local charge. The electron conductivity of the cation B lattice is obtained from B-O-B bonding by Zerner double exchange mechanism as shown in the following reaction:

$$B^{n+} - O^{2-} - B^{(n+1)+} \rightarrow B^{(n+1)+} - O^{-} - B^{(n+1)+} \rightarrow B^{(n+1)+} - O^{2-} - B^{n+} \quad (2)$$

The oxygen ion is then oxidized to oxygen on the surface of the membrane which then desorption in the form of gas (Shao et al., 2000). Therefore, the description of the fundamental theory on perovskite crystal structure, various synthesis methodology, and the performance of the perovskite oxide is important to be declared in this brief review.

Crystal structure of perovskite oxides

Further studies reported a change in perovskite crystal structure from cubic to pseudo-cubic such as rhombohedral (R3c), orthorhombic and hexagonal. Table 1 showed different lattice parameters which were identified by x-ray diffraction (XRD) instrument or high-temperature x-ray diffraction (HT-XRD) to enhance the higher resolution result of the crystal data. Then the data were fitted with Inorganic Crystal Structure Database (ICSD) and calculated using RIETICA software as a Rietveld refinement method. The calculation result must be under the Goodness of Fit (GoF) value then the lattice parameter can be reported.

Cheng et al. (2015) reported $Bi_{0.7}Pr_{0.1}Ba_{0.2}FeO_3$ which was synthesized by conventional solid-state method at a temperature of 880 °C for 1 h showed that no unit cell change during the calcination process due to the substitution of Ba and Pr improved the structural stability. $BiFeO_3$ as the main crystal structure before the substitution had a low electrical performance which was caused by the distorted rhombohedral metastable structure. The effect of metal ion substitution also

changed the unit cell of $CaTiO_3$. $Ca_2Fe_2O_5$. $CaMnO_3$ dan $CaZrO_3$ (Kesić et al., 2016). Thus, the different structures led to different performances as mentioned above.

$Ca_{1/3}La_{2/3}MnO_3$ perovskite was successfully synthesized by a mechanochemical method which no calcination occurs in this process. The result showed that different milling times for 0.5; 3; 4.5 and 9 h changed especially at 3 and 9 h. These unit cell differences did not produce different structures. While the milling time using planetary ball mill for 0.5 h occurred no characteristic peaks at the diffractogram. This suggests that unit cell changes are influenced by the energy from stirring ball during the mechanochemical process (Bolarín et al., 2007). The Rietveld refinement method was also able to find other phases which formed in the material, as in Blanchard et al's study for $(Bi_{0.5}Na_{0.5})$ TiO_3 material (Blanchard *et al.*, 2014).

Table 1. Perovskite oxide structure

Materials	Space Group	Unit cells (Å)			Ref
		a	B	c	
$Bi_{0.7}Pr_{0.1}Ba_{0.2}FeO_3$	Pm3m	3.97809(84)	3.97809(84)	3.97809(84)	(Cheng et al., 2015)
$Ca_{1/3}La_{2/3}MnO_3$ (3 h)	Pbnm	5.476±0.004	5.519±0.004	7.704±0.004	(Bolarín et al., 2007)
$Ca_{1/3}La_{2/3}MnO_3$ (9 h)		5.474±0.003	5.488±0.018	7.769±0.033	
$CaTiO_3$	Pbnm	5.3827	5.4537	7.6551	(Kesić et al., 2016)
$Ca_2Fe_2O_5$	Pcmn	5.5946	14.8273	5.4307	
$CaMnO_3$	Pnma	5.2770	7.4510	5.2643	
$CaZrO_3$		5.7515	8.0138	5.5922	
$(Bi_{0.5}Na_{0.5})$ TiO_3	Cc-R3c	9.5087(8) 5.4916(6)	5.4829(5) 5.4916(6)	5.5176(5) 13.4921(16)	(Blanchard et al., 2014)

Synthesis of perovskite oxides

Perovskite oxides properties can be improved through several modifications such as the synthesis method, which is the first step and very important in the preparation process. Particularly synthesize methods were mostly divided by four, they are solid-state, sol-gel, combustion, and co-precipitation (Liu et al., 2009; Zou et al., 2011). The different synthesis methods have significant effects on material properties such as $PrBaCo_2O_{5+\delta}$ in Table 2.

$PrBaCo_2O_{5+\delta}$ was successfully synthesized by solid-state, sol-gel, combustion, and pechini methods. Solid-State and Pechini methods were applied at the same sintering temperature but they showed different lattice parameters. In addition, the number of 5+δ using the sol-gel method is also the lowest that indicating its lower ionic conductivity compared to the other methods used. Therefore, further information will be explained.

Table 2. $PrBaCo_2O_{5+\delta}$ synthesize using different methods

Material	Methods	Temp (^{0}C)	a (Å)	b (Å)	c (Å)	5+δ	Ref
$PrBaCo_2O_{5+\delta}$	Solid state	1100	3.902	3.906	7.631	5.70	(Maignan et al., 1999)
	Sol-gel	1000	3.909	-	7.638	5.64	(Jiang et al., 2014)
	Combustion	950	3.868	3.871	7.576	5.79	(Zhao et al., 2011)
	Pechini	1100	3.915	3.902	7.699	5.78	(Park et al., 2012)

Solid-state method

The solid-state method is a conventional solid-solid reaction with no solvent then calcined at high temperature to form perovskite oxide. As the most common method, the methodology firstly prepares the precursors which can be from a metal oxide, nitrate, and carbonate (Zou et al., 2011) with a mass ratio following the stoichiometry and a dispersant such as methanol or isopropanol to increase the homogeneity of the particle size (Fansuri et al., 2015). The solid-state method results in low particle size homogeneity although this method is considered a more favorable step due to the efficiency process and no solvent which produces a high purity of perovskite phase (Zhou et al., 2009).

Firstly, the precursors are weighed based on the stoichiometric ratio. Then it is milled mechanically for 3 to 24 h, next calcined at a temperature of 800-1000 °C for 5 to 48 h (Song et al., 2015). The calcination is applied to enhance the cation mobility which is diffused and reacted with other cation ions of the precursors (Athayde et al., 2015). The sintering process affects the ion diffusion as shown in Figure 2 which is the mobility of the cations through the crystalline to form perovskite. Other factors initiated its characteristic. They are metal precursors, milling process, and sintering.

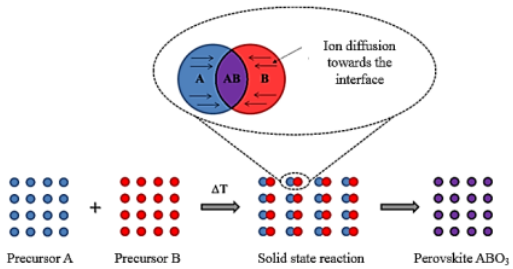

Figure 2. Schematic of ion diffusion process from precursors to perovskite formation using solid-state reaction (Athayde et al., 2015).

A variety of precursors as mentioned above, metal oxides precursors are mostly used due to high cation mobility compared sequentially to metal carbonate and nitrate. Even though metal nitrate is known as a hygroscopic which affects the stoichiometry calculations. Fansuri et al. (2015)was successfully synthesized LSCF 7328 using strontium nitrate ($Sr(NO_3)_2$) as a precursor. The diffractogram showed in Figure 3 matched with standard data as mentioned although the Co_3O_4 phase at 37° was ignored due to a very small peak and no nitrate phase appeared in the diffractogram.

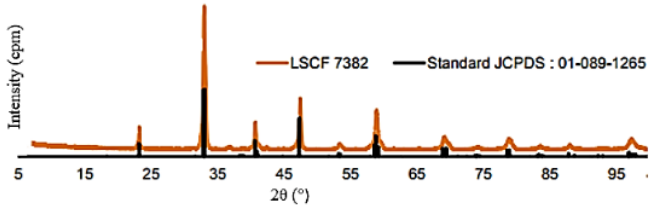

Figure 3. Diffractogram of LSCF 7328 (Fansuri et al., 2015).

Based on the mechanochemical for cation mobility as the point of view, the milling process significantly has an important effect such as rational speed varied from 300 to 600 rpm and milling time for 2 until 6 h (da Côrte et al., 2013). da Côrte et al reported that the secondary phases were shown using 300 rpm, indicating that oxide precursors are still present at low rotational speed as well as the milling time duration. The crystallite of LSCF can be synthesized at a minimum of 500 rpm for 4 h milling. However, they did not provide a detailed description using 600 rpm. Wang et al (Wang et al., 2011) investigated the effect of milling time on resistivity as shown in Figure 4.

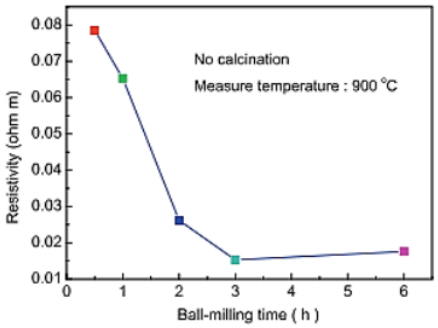

Figure 4. Effect of Milling Process on Resistivity (Wang et al., 2011).

By increasing milling time it was found that the resistivity of $La_{0.8}Sr_{0.2}MnO_3$ dropped sharply due to an increase in the rate of perovskite formation. The low resistivity indicated more electron holes formation then increase the electron flow through the lattice of the structure. In the same research report, sintering is the last step but very important to increase the dense, physical, and chemical properties such as the resistivity decreased by increasing sintering temperature up to 1200 °C for 10 h in LSM formation which was different with Wang et al (Wang et al., 2014) result by using sintering temperature 1200 °C for 4 h in $La_{0.7}Sr_{0.3}Mn_{1-x}Fe_xO_{3\pm\delta}$. The XRD pattern showed a sharp peak which indicated the pure phase of the perovskite.

The different sintering temperatures was depended on the decomposition temperature of the material such as da Côrte et al's thermogram of LSCF powder as shown in Figure 5 (da Côrte et al., 2013). The first stage indicated the loss of water and carbon dioxide at 400 °C then 550-800 °C showed complete decomposition of carbonate which can be initiated calcination temperature although the higher temperature was also needed for perovskite densification. Therefore, the solid-state method is simple and has low operational cost as well as high phase purity. Even though directly obtained the particle and grain size which approximately 1-2 μm. By using continuous milling, finer powders with lower particle sizes can be obtained.

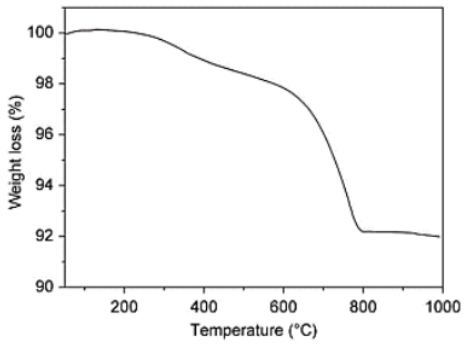

Figure 5. Thermogram of LSCF powder prepared by solid-state method (da Côrte et al., 2013).

Sol-gel method

Sol-gel is the accurate method to control the final material composition with a low particle size around 10 nm (Athayde et al., 2015). Generally, the step begins with the preparation of sol from metal precursors and chelating agents to prevent the segregation of the metal precursors which the ratio plays an important role to delivers the homogeneous solution. Then the hydrolysis process is occurred to for.

m metal-oxygen-inorganic metal bonding by water or organic solvent solution. Next, and the condensation process is applied to form a gel which is subsequently dried at a temperature of less than 100 °C to intermediate temperature 350 °C (Cot et al., 2000). In the other words, sol as solid particles with a diameter of 1-100 nm in a liquid can be derived to some gel types which has different application such as the coating on the dense film, gelling to form dense ceramic and aerogel, precipitating to form uniform particles and spinning to form ceramic fibers (Hench & West, 1990).

$La_{0.75}Sr_{0.25}Cr_{0.5}Mn_{0.5}O_{3-\delta}$ was successfully synthesized using the sol-gel method by modification of ethylene-diamine-tetra acetate acid (EDTA) usage as a chelate agent. The result showed that the chelating agent of EDTA resulted from stronger bonding afer organic compounds removal. Besides EDTA usage, EDTA-citrate, oxalic acid, and citric nitrate are suitable to be chelating agents due to they have electron-donating groups, carboxylic acid, and aliphatic amine as be seen in **Error! Reference source not found.** 6 (Wan et al., 2006).

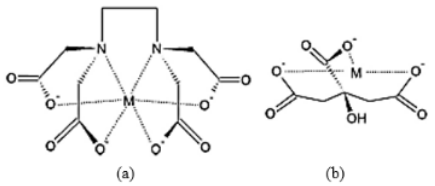

Figure 6. Complexes formed between the metal ion and EDTA (a) and citric acid (b) as chelating agents (Athayde et al., 2015).

Combustion method

The combustion method begins with metal nitrates as a precursor which is weighed based on a stoichiometric ratio. The advantage of this method is obtaining uniform particle size, homogeneous particle, effective and fast process, and also low operational cost (Nuernberg & Morelli, 2016). Generally, the precursor is used in nitrate form, ethylene glycol, citric acid, ammonia and water. The citric acid serves as a chelate and reducing agent while ammonia is used

to pH control until it reaches the perfect citric acid complex with a metal ion without any precipitated compounds. In addition, ethylene glycol is used as a gel-forming agent that will facilitate the combustion process.

Both sol-gel and combustion can be combined as a novel perovskite synthesis method which had been reported by Guo et al (Guo et al., 2006). They had succeeded in $La_{0.7}Sr_{0.3}MnO_3$ synthesis using the gel combustion method with a variation of pH value and citric acid concentration. Metallic ions are reacted with COO- in solution to form metal-citrate complexes. The pH value will be affected the dissociation of the complex of citric acid and metals and does not produce a precipitate. This is evidenced by the value of ionized La^{3+}. Mn^{2+} and Sr^{2+} + to the pH value shown in Figure 7. The results showed that all three metal ions formed perfectly complex at a certain pH of La^{3+} at pH 1.5, Mn^{2+} at pH 3.5, and Sr^{2+} at pH 4. Therefore, the optimal pH used is less than 4 to avoid the formation of soles on the mixture of precursors.

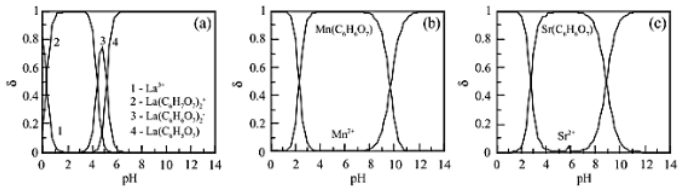

Figure 7. The Effect of Different pH Number on La^{3+}. Mn^{2+} dan Sr^{2} Ion Distribution (Guo et al., 2006).

Unfortunately, the procedures were not simple which the propagation combustion must be regularly recorded during the sintering process with dependent temperature by its synthesized material. After the ignition process occurs, the powders were heated up to 600 °C for 1 h.

Co-precipitation method

The co-precipitation method is used for obtaining nano-sized perovskite oxides. The basic principle of this method is the precipitation of more than one substance together after passing through the saturation point. The advantage of the co-precipitation method is the use of low synthesis temperature, easy to control particle size, high homogeneity, and high purity. Herein, the parameters which can help control the desired material are temperature, stirring speed, pH value, washing process, and concentration of the precursors with general schematic is shown in Figure 7 (Athayde et al., 2015).

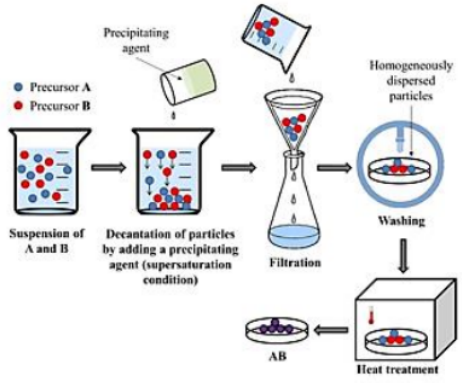

Figure 7. General schematic of co-precipitation method (Athayde et al., 2015)

The steps of the method generally begin with the selection of precursors derived mostly from nitrate salts. The precursor was then dissolved in distilled water and added 1 M Na_2CO_3 to pH 10 with constant stirring. After that, the aging process for 30 minutes at room temperature and was washed with water until the pH reaches 7. Dried for 24 hours at 100 ° C and calcined at 750 ° C for 5 hours. One of the materials that have been successfully synthesized using the co-precipitation method is $LaCoO_3$ and $La_{0.8}Sr_{0.2}CoO_3$ which produce a specific surface area of 2.60 m^2g^{-1} and 5.31 m^2g^{-1}, respectively (Patel & Patel, 2013).

Mostafavi et al (Mostafavi et al., 2015) reported that the most important parameter to synthesis $La_{0.6}Sr_{0.4}Co_{0.2}Fe_{0.8}O_3$ (LSCF) using the co-precipitation method was the pH control due to the secondary phase commonly appearing such as cobalt ferrite ($CoFe_2O_4$) at unsuitable pH. The pH can be changed by different precipitation agent usage which the carefulness of its concentration is also very important. Figure 8 showed the influence of different precipitation agents of precursors on the phase formation. The precipitation by ammonium carbonate (NH_4^+/NO_3^-) provides higher stability of pH in metal nitrate solution as well as the homogeneity of the solution compared to sodium hydroxide (NaOH) as a precipitation agent. In addition, the second phase such as La_2O_3 was also found when the destined water was used to simply wash at room temperature then calcined to form a high purity phase of LSCF perovskite with an optimized temperature of 1000 °C.

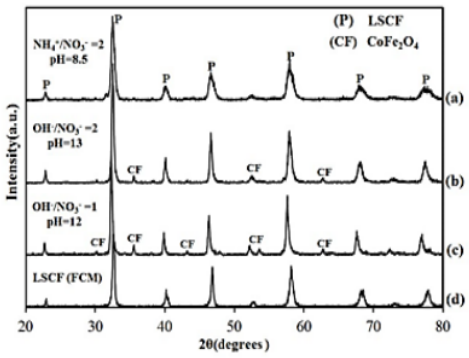

Figure 8. Diffractogram of Calcined LSCF by NH_4^+/NO_3^- =2 (pH=8.5) (a), OH^-/NO_3^- =2 (pH = 13) (b) and OH^-/NO^- = 1 (pH=12 (c)) then Calcined at 1000 °C for 1 h and A Commercial LSCF Powder (d).

In conclusion, perovskites are a very interesting, diverse group of materials, exhibiting a wide range of useful properties defined by their composition. Oxygen vacancy in its structure leads to many functions as a catalyst or MIEC characterization with the capability to transport oxygen ions and electrons in opposite directions, thus the synthesis method is also important to be considered because of these different characteristic products from different syntheses methods. Solid-state method, although it produces not a small particle size but its simple procedure and no emission of pollutants as much as the wet method. The sol-gel method can produce perovskite oxide powders in size up to nanometer but it releases many pollutants due to the use of sol-gel forming agents as well as combustion and co-precipitation method.

Perovskite membrane performance

Perovskite oxide as anionic and electronic conductors was originally used as a cathode on solid oxide fuel cells (SOFC) at low temperatures then developed for methane conversion catalyst at high temperature >900 °C (Murata et al., 2005; Shen et al., 2010). The value of an ionic

conductivity (σ_{ion}) indicates the permeability of oxygen which able to pass through the lattice of perovskite oxide structure and can be calculated using the following equation:

$$\sigma_{ion} = \left(\frac{C}{T}\right) \exp\left(\frac{-E_a}{K'T}\right) \quad (3)$$

Where the Ea value is equivalent to the average value of bonding energy between metal-oxygen. The low value of Ea shows increasing in ionic conductivity, then C is a constant value which indicates the oxygen vacancy of the lattice structure (Shao et al., 2000). The electronic conductivity (σ_e) also can be calculated using the same eq 3 (da Conceição et al., 2009).

While the volume value of oxygen per unit time and membrane area is expressed as oxygen flux which can be determined using eq 4

$$J_{O_2} = \frac{FC_{O_2}}{S} \quad (4)$$

Where J_{O_2} is an oxygen permeation flux (mL.min^{-1}.cm^{-2}) which is measured using He as a sweep gas with flow rate F (mL.min^{-1}). Furthermore, the oxygen concentration passes through the membrane as C_{O_2}(%) and the specific surface area is S (cm^2).

The use of carrier gas affects the value of oxygen permeation flux due to each sweep gas has a different conductivity value. When He is used as a carrier gas, the concentration of oxygen vacancies on the surface is only related to the partial pressure of oxygen on each side of the membrane. If the CO_2 is used to carrier gas, the possible chemical adsorption will occur to the membrane surface with oxygen ions in CO_2 occupying the vacancy side of oxygen in the membrane. Therefore, the concentration of oxygen vacancies through the membrane will decrease and produce a negative impact on the perovskite membrane. While the largest permeation flux can be achieved by using H_2 or He as a carrier. The use of H2 as a carrier will not affect good measurement when the membrane is used for POM reaction catalyst which will produce H_2 as its product (Jin et al., 2016; Tan et al., 2012).

If some lattice oxygen has a slow reaction rate to pass through the membrane on another side then the lattice oxygen will return to the reverse side by bringing the oxygen vacancy side. The oxygen permeation flux of a perovskite material also becomes one of the determinants of high or low catalytic performance. In POM reaction, oxygen permeation flux is measured at a high temperature of about 1000 ° C because POM reaction applications require high temperatures to activate the methane bonding.

Therefore, perovskite membranes are utilized as catalysts as well as oxygen suppliers in POM reactions. The POM reaction using perovskite membrane is illustrated as in Figure 9 which occurs only on the membrane surface which further oxidation cannot be allowed on POM reaction catalyst because the perovskite oxide catalyst membrane is only capable of being penetrated by oxygen ion (Sokolovskii et al., 1998).

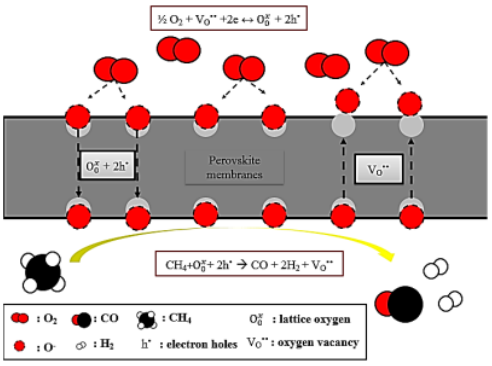

Figure 9. Partial oxidation process using perovskite oxide catalyst.

One of the most widely studied perovskite types of the cobalt-based methane oxidation reaction is $LaCoO_3$ (Teraoka et al., 1991). The substitution of La^{3+} by Sr^{2+} ion and the substitution of Co^{3+} by Fe^{3+} ion can increase the value of structural stability. The perovskite oxide containing La and Sr on the A and Co and/or Fe sides on the B-side is known as the cathode material candidate for the IT-SOFCs because it produces a high value of ionic and electronic conductivity, also the oxygen catalytic activity. However, the compound with Co on the B side is very easy to react with YSZ which increases the resistance to the cathode surface. A high resistance value will reduce the oxygen permeation flux.

The target resistance value for a good SOFCs application is less than 1.5 $\Omega.cm^2$ which can produce good oxygen permeation flux (Murata et al., 2005). The electronic and ionic conductivity values are expected to be high so that they can be correlated for POM reaction applications. The perovskite oxide of $(LaSr)(CoFe)O_3$ (LSCF) and $LaSrMnO_3$ (LSM) are good candidates for SOFCs cathodes because they have good electron conductors, high stability, and high electrochemical activity for the reduction of oxygen at high temperatures (Jiang. 2002). In a previous study, the amount of Sr^{2+} ions will result in a decrease in the number of oxygen ions attached to the crystal lattice of the perovskite (Wei et al., 2008).

Conclusion

In conclusion, perovskite oxide has a distinctive crystal structure, namely the presence of oxygen vacancy to increase the effectiveness in separating oxygen from the air. The existence of variations in metal types on the A and B sides, and the synthesis method have a significant influence on their physical and chemical properties. The choice of the type of metal that fills the sides (A and B side) of the crystal structure is adjusted to the radius of the metal ion that can survive in the range governed by the Goldsmith equation, as the structural tolerance equation for typical perovskite oxides. Synthetic methods that have been successful in the manufacture of perovskite oxide powder are solid-state, sol-gel, combustion, and co-precipitation. The different methods applied have a significant impact on particle size and shape, crystallographic properties, yield, active surface area, and performance in separating oxygen from the air. Therefore, researchers can adapt the application of the synthesis method to the needs of the perovskite properties. Some applications that can utilize perovskite oxide are syngas production from methane, solid oxide fuel cell (SOFC), methanol production from methane, etc.

Acknowledgment

The authors would like to thank to the Faculty of Technology, Universitas Pembangunan Nasional "Veteran" Jawa Timur and DIPA Universitas Pembangunan Nasional "Veteran" Jawa Timur for the financial support.

References

Athayde, D. D., Souza, D. F., Silva, A. M. A., Vasconcelos, D., Nunes, E. H. M., Costa, D.d., & Vasconcelos, W. L. (2015). Review of perovskite ceramic synthesis and membrane preparation methods. *Ceramics International*, *42*(6), 6555–6571. doi: https://doi.org/10.1016/j.ceramint.2016.01.130.

Blanchard, P. E. R., Liu, S., Kennedy, B. J., Ling, C. D., Zhang, Z., Avdeev, M., Jang, L.-Y., Lee, J.-F., Fao, C-W., & Chen, J-L. (2014). Studying the effects of Zr-doping in (Bi0.5Na0.5)TiO3 via diffraction and spectroscopy. *Dalton Transactions*, 43(46), 17358. DOI:10.1039/c4dt02520b

Bolarín, A. M., Sanchez, F., Palomares, S., Aguilar, J. A., & Torres-Villasenor, G. (2007). Synthesis of calcium doped lanthanum manganite by mechanosynthesis', *Journal of Alloys and Compounds*, *436*(1–2), 335–340. http://dx.doi.org/10.1016%2Fj.jallcom.2006.07.061

Cheng, G. F., Ruan, Y. J., Liu, W., & wu, X. S. (2015). Effect of temperature on structural expansion for Bi0.8-xPrxBa0.2FeO3 (x <= 0.1) ceramics. *Thermochimica Acta*, *602*, 74–77.

da Conceição, L., Silva, C. R. B., Ribeiro, N. F. P., & Souza, M. M. V. M. (2009). Influence of the synthesis method on the porosity, microstructure and electrical properties of La0.7Sr0.3MnO3 cathode materials. *Materials Characterization*, *60*(12), 1417–1423. doi: 10.1016/j.matchar.2009.06.017.

da Côrte, R. V., da Conceição, L., & Souza, M. M. V. M. (2013). Structural and electrical properties of La0.7Sr0.3Co0.5Fe0.5O3 powders synthesized by solid state reaction', *Ceramics International*, *39*(7), 7975–7982. doi: 10.1016/j.ceramint.2013.03.063.

Cot, L., Ayral, A., Durand, J., Guizard, C., Hovnanian, N., & Julbe, A. (2000). Inorganic membranes and solid state sciences. *Solid State Sciences*, 2(3), 313–334. Doi:10.1016/S1293-2558(00)00141-2

Fansuri, H. et al. (2015). Determination of oxygen flux on flat membranes made of La0,7Sr0,3Co0,8Fe0,2O3 and Ba0,5Sr0,5Co0,8Fe0,2O3 perovskite oxide. in *SEMIRATA 2015 bidang MIPA BKS-PTN Barat*. Pontianak: Universitas Tanjungpura, pp. 670–679.

Guo, R. S., Wei, Q. T., Li, H. L., & Wang, F. H. (2006). Synthesis and properties of La0.7Sr0.3MnO3 cathode by gel combustion. *Materials Letters*, *60*(2), 261–265. http://dx.doi.org/10.1016%2Fj.matlet.2005.08.027

Hench, L. L., & West, J. K. (1990). The sol-gel process. *Chemical Reviews*, *90*(1), 33–72. doi: 10.1021/cr00099a003.

Jiang, L., Li, F. S., Wei, T., Zeng, R., & Huang, Y. H. (2014). Evaluation of Pr1+xBa1-xCo2O5+δ (x = 0 - 0.30) as cathode materials for solid-oxide fuel cells. *Electrochimica Acta*, *133*(0), 364–372. Doi: 10.1016/j.electacta.2014.04.064

Jiang, S. P. (2002). A comparison of O 2 reduction reactions on porous (La,Sr)MnO3 and (La,Sr)(Co,Fe)O 3 electrodes. *Solid State ionics*, *146*, 1–22.

Jin, Y., Meng, X., Meng, B., Yang, N., & Zhang, C. (2016). Simulation of oxygen permeation through La0.6Sr0.4Co0.2Fe0.8O3−δ tubular membrane reactor with POM reactions. *International Journal of Hydrogen Energy*, *41*(39), 2–10. Doi:10.1016/j.ijhydene.2016.07.076

Kesić, Ž., Likic, I., Zdujic, M., Jovalekic, C., Veljkovic, V. B., & Skala, D. (2016). Assessment of CaTiO3, CaMnO3, CaZrO3 and Ca2Fe2O5 perovskites as heterogeneous base catalysts for biodiesel synthesis. *Fuel Processing Technology*, *143*, 162–168. Doi:10.1016/j.fuproc.2015.11.018

Liu, H., Pang, Z. B., Tan, X., Shao, Z., Sunarso, J., Ding, R., & Liu, S. (2009). Enhanced oxygen permeation through perovskite hollow fibre membranes by methane activation. *Ceramics International*, *35*(4), 1435–1439. Doi:10.1016/j.ceramint.2008.07.011

Maignan, A., Martin, C., Pelloquin, D., Nguyen, N., & Raveau, B. (1999). Structural and Magnetic Studies of Ordered Oxygen-Deficient PerovskitesLnBaCo2O5+δ, Closely Related to the "112" Structure. *Journal of Solid State Chemistry*, *142*(2), 247–260.

Möbius, A., Henriques, D., & Markus, T. (2009). Sintering behaviour of La1-xSrxCo0.2Fe0.8O3-δ (0.3 ≤ x ≤ 0.8) mixed conducting materials. *Journal of the European Ceramic Society*, 29(13), 2831–2839.

Mostafavi, E., Babaei, A., & Ataie, A. (2015). Synthesis of nano-structured La0.6Sr0.4Co0.2Fe0.8O3 perovskite by co-precipitation method. *Journal of Ultrafine Grained and Nanostructured Materials*, *48*(1), 45–52.

Murata, K., Fukui, T., Abe, H., Naito, M., & Nogi, K. (2005). Morphology control of La(Sr)Fe(Co)O3−α cathodes for IT-SOFCs. *Journal of power sources*, *145*(2), 257–261. Doi:10.1016/j.jpowsour.2004.12.063

Nuernberg, R. B., & Morelli, M. R. (2016). Synthesis of BSCF perovskites using a microwave-assisted combustion method. *Ceramics International*, *42*(3), 4204–4211. 10.1016/j.ceramint.2015.11.094

Park, S., Choi, S., Kim, J., Shin, J., & Kim, G. (2012). Strontium doping effect on high-performance PrBa1-xSrxCo2O5+δ as a cathode material for IT-SOFCs. *ECS Electrochemistry Letters*, *1*(5), F29–F32. doi: doi: 10.1149/2.007205eel.

Patel, F., & Patel, S. (2013). 'La1-xSrxCoO3 (x=0, 0.2) perovskites type catalyst for carbon monoxide emission control from auto-exhaust', *Procedia Engineering*, *51*(NUiCONE 2012), pp. 324–329.

Shao, Z., Xiong, G., Cong, Y., & Yang, W. (2000). Synthesis and oxygen permeation study of novel perovskite-type BaBixCo0.2Fe0.8−xO3−δ ceramic membranes. *Journal of Membrane Science, 164* (s1-2), 167–176. doi: doi.org/10.1016/S0376-7388(99)00211-2.

Shen, Z., Lu, P., Hu, J., & hu, X. (2010). Performance of Ba0.5Sr0.5Co0.8Fe0.2O3+δ membrane after laser ablation for methane conversion. *Catalysis Communications*, *11*(10), 892–895.

Sokolovskii, V. D., Coville, N., Parmaliana, A., Eskendirov, I., & Makoa, M. (1998). Methane partial oxidation. challenge and perspective. *Catalysis Today*, *42*(3), 191–195. Doi:10.1016/S0920-5861(98)00091-1

Song, S., Zhang, P., Zhang, X., & Han, M. (2015). Partial oxidation of methane reaction in Ba0.9Co0.7Fe0.2Nb0.1O3-δ oxygen permeation membrane with three-layer structure. *International Journal of Hydrogen Energy*, *40*(34), 10894–10901. Doi:10.1016/j.ijhydene.2015.06.134

Tan, X., Liu, N., Meng, B., Sunarso, J., Zhang, K., & Liu, S. (2012). Oxygen permeation behavior of La0.6Sr0.4Co0.8Fe0.2O3 hollow fibre membranes with highly concentrated CO2 exposure. *Journal of Membrane Science*, *389,* 216–222. Doi:10.1016/j.memsci.2011.10.032

Teraoka, Y., Nobunaga, T., Okamoto, K., Miura, N., & Yamazoe, N. (1991). Influence of constituent metal cations in substituted LaCoO3 on mixed conductivity and oxygen permeability. *Solid State Ionics*, *48*(3–4), 207–212.

Wan, J., Zhu, J. H., & Goodenough, J. B. (2006). La0.75Sr0.25Cr0.5Mn0.5O3-δ + Cu composite anode running on H2 and CH4 fuels', *Solid State Ionics*, 177(13–14), 1211–1217.

Wang, B., Cao, Q., & Zhang, S. (2014). Effects of the incorporation of Fe on the electromagnetic and microwave absorption performance of La0.7Sr0.3MnO 3±δ', *Materials Science in Semiconductor Processing*, *19*(1), 101–106. doi: 10.1016/j.mssp.2013.12.010.

Wang, M., Woo, K. Do, & Lee, C. G. (2011). Preparing La0.8Sr0.2MnO3 conductive perovskite via optimal processes: High-energy ball milling and calcinations. *Energy Conversion and Management*, *52*(3), 1589–1592.

Wei, H. J., Cao, Y., Ji, W. J., & Au, C. T. (2008). Lattice oxygen of La1-xSrxMO3 (M = Mn, Ni) and LaMnO3-a perovskite oxides for the partial oxidation of methane to synthesis gas. *Catalysis Communications*, *9*(15), 2509–2514. doi: 10.1016/j.catcom.2008.06.019.

Teraoka, Y., Zhang, H. M., Furukawa, S., & Yamazoe, N. (1985). Oxygen permeation through pervoskite-type oxides. *Chemistry Letters*, (C), 1743–1746.

Zhao, L., Shen, J., He, B., Chen, F., & Xia, C. (2011). Synthesis, characterization and evaluation of PrBaCo2−xFexO5+δ as cathodes for intermediate-temperature solid oxide fuel cells. *International Journal of Hydrogen Energy*, *36*(5), 3658–3665. Doi:10.1016/j.ijhydene.2010.12.064

Zhou, W., Ran, R., & Shao, Z. (2009). Progress in understanding and development of Ba0.5Sr0.5Co0.8Fe0.2O3-δ-based cathodes for intermediate-temperature solid-oxide fuel cells: A review. *Journal of Power Sources*, *192*(2), 231–246.

Zou, Y., Zhou, W., Liu, S., & Shao, Z. (2011). Sintering and oxygen permeation studies of La0.6Sr0.4Co0.2Fe0.8O3-δ ceramic membranes with improved purity. *Journal of the European Ceramic Society*, *31*(15), 2931–2938.

04. Brief Overview of Perovskite Oxide: Synthesis and Its Performance as Oxygen Separator from Air

ORIGINALITY REPORT

3%	%	%	3%
SIMILARITY INDEX	INTERNET SOURCES	PUBLICATIONS	STUDENT PAPERS

PRIMARY SOURCES

1	Submitted to Universitas Mataram Student Paper	1%
2	Submitted to Higher Education Commission Pakistan Student Paper	1%
3	Submitted to Swinburne University of Technology Student Paper	<1%
4	Submitted to The University of the South Pacific Student Paper	<1%
5	Submitted to Universiti Teknologi Malaysia Student Paper	<1%
6	Submitted to 13567 Student Paper	<1%

Exclude quotes	Off	Exclude matches	Off
Exclude bibliography	On		